



1

1 **The Ant-Iso dataset: a compilation of Antarctic surface snow isotopic**  
2 **observations**

3

4 Jiajia Wang<sup>1</sup>, Hongxi Pang<sup>1</sup>, Shuangye Wu<sup>2</sup>, Spruce W. Schoenemann<sup>3</sup>, Ryu Uemura<sup>4</sup>,  
5 Alexey Ekaykin<sup>5,6</sup>, Martin Werner<sup>7</sup>, Alexandre Cauquoin<sup>8</sup>, Sentia Goursaud Oger<sup>9,\*</sup>,  
6 Summer Rupper<sup>10</sup>, and Shugui Hou<sup>1,11</sup>

7

8 <sup>1</sup>Key Laboratory of Coast and Island development of Ministry of Education, School of Geography and  
9 Ocean Science, Nanjing University, Nanjing, China

10 <sup>2</sup>Department of Geology and Environmental Geosciences, University of Dayton, Dayton, USA

11 <sup>3</sup>Environmental Sciences Department, The University of Montana Western, Dillon, MT, 59725, USA

12 <sup>4</sup>Graduate School of Environmental Studies, Nagoya University, Furo-cho, Chikusa-ku, Nagoya,  
13 464-8601, Japan

14 <sup>5</sup>Climate and Environmental Research Laboratory, Arctic and Antarctic Research Institute, 38 Beringa  
15 st., 199397 St. Petersburg, Russia

16 <sup>6</sup>St. Petersburg State University, 33–35, 10th line VO, 199178 St. Petersburg, Russia

17 <sup>7</sup>Alfred Wegener Institute, Helmholtz Centre for Polar and Marine Sciences, Bremerhaven, Germany

18 <sup>8</sup>Institute of Industrial Science (IIS), The University of Tokyo, Kashiwa, Japan

19 <sup>9</sup>Department of Earth Sciences, University of Cambridge, Cambridge, UK

20 <sup>10</sup>Department of Geography, University of Utah, Salt Lake City, UA, United States

21 <sup>11</sup>School of Oceanography, Shanghai Jiao Tong University, Shanghai, China

22 \* Currently CEA, DAM, DIF, F-91297 Arpajon, France

23  
24 Correspondence to: Hongxi Pang (email: hxpang@nju.edu.cn) and Shugui Hou (email:  
25 shuguihou@sjtu.edu.cn)

26 **Abstract.** Stable water isotopic observations in surface snow over Antarctica  
27 provide a foundation for validating isotopic models and interpreting Antarctic ice core  
28 records. Here, we present a new compilation of Antarctic surface snow isotopic



2

29 dataset with strict quality control from published and unpublished sources including  
30 measurements from snow pits, snow cores, ice cores, deep surface snow, and  
31 precipitation (multi-year average values). The dataset contains a total of 1867 data  
32 points, including 1604 locations for oxygen isotope ratio ( $\delta^{18}\text{O}$ ) and 1278 locations  
33 for deuterium isotope ratio ( $\delta^2\text{H}$ ). 1204 locations have both  $\delta^{18}\text{O}$  and  $\delta^2\text{H}$ , from which  
34 d-excess ( $\text{d-excess} = \delta^2\text{H} - 8 \times \delta^{18}\text{O}$ ) can be calculated. The dataset also contains  
35 geographic and climate information. The database has a wide range of potential  
36 applications, such as the study of the spatial distribution of water isotopes in  
37 Antarctica, the evaluation of climate models, and the reconstruction and interpretation  
38 of Antarctic ice core records. As an example of model evaluation, the compiled  
39 isotopic dataset is used to assess the performance of isotope-enabled atmospheric  
40 general circulation models (AGCMs) on simulating the spatial distribution of water  
41 isotopes over Antarctica. This dataset is the most comprehensive compilation so far of  
42 observed water isotope records at multi-year average scale from multiple sources for  
43 Antarctica. It is available for download at <https://doi.org/10.5281/zenodo.7294183>  
44 (Wang et al., 2022).

45

## 46 **1 Introduction**

47 Under the current global warming, changes in the Antarctic continent and ice sheet  
48 have profound impacts on the global sea level, the atmospheric circulation, and many  
49 other important aspects of the Earth systems (Medley and Thomas, 2019; Naughten et  
50 al., 2021; Stokes et al., 2022). To better understand and predict climate change in  
51 Antarctica, it is important to investigate its past variations, which is limited by the  
52 length of instrumental data (reanalysis data and automatic weather station), covering  
53 only about 60 years. Therefore, assessing long-term climate change in Antarctica



3

54 requires climate proxy records. Ice cores from Antarctica are critical archives for  
55 climate change due to their high resolution, long temporal coverage, large amount of  
56 information, and high fidelity. As one of the most important ice core records, the  
57 stable water isotopic record is used to reconstruct past temperatures and provides a  
58 fundamental understanding on past climate change (Brook and Buizert, 2018; Buizert  
59 et al., 2021; Jouzel et al., 2007).

60 Conventional temperature reconstructions by stable water isotopic records in ice  
61 cores rely on the empirical spatial linear relationship between the isotopic  
62 composition in surface snow and air temperature. The establishment of such  
63 relationship requires sufficient observational data. Despite the large number of  
64 isotopic observations made in Antarctica over the past few decades, the spatial  
65 coverage is still uneven. Masson-Delmotte et al. (2008, hereafter MD08) compiled the  
66 first multi-year-averaged Antarctic surface snow stable isotope dataset, which  
67 provided a solid foundation for related research on Antarctic water isotope  
68 climatology. First, it provides an observational basis for numeric simulations of the  
69 spatial distribution of snow isotopes across Antarctica using pure mathematical  
70 methods combined with high-resolution digital elevation models (Hatvani et al., 2017;  
71 Wang et al., 2009a, 2009b, 2010). Second, it can be used to reconstruct  
72 paleo-temperature and paleo-elevation changes (Werner et al., 2018). Finally, the  
73 database can be used as a benchmark to evaluate isotope-enabled atmospheric general  
74 circulation models (AGCMs) and Rayleigh distillation isotope models.

75 Although isotopic observations have been recorded at over one thousand sampling  
76 sites, the spatial coverage of isotope data remains highly uneven (MD08). Only a few  
77 data are available on the West Antarctic Ice Sheet and at high altitudes of the East  
78 Antarctic interior regions. After the pioneering work of MD08, numerous new



4

79 samples and measurements have been acquired by different researchers. Incorporating  
80 these additional observations, we have recompiled the most comprehensive Antarctic  
81 surface snow isotopic dataset, which significantly increases the spatial coverage  
82 relative to the MD08. This article aims to provide some details on the collection of the  
83 isotopic measurements used to produce this updated Antarctic surface snow isotopic  
84 dataset, including data sources, data spatial distribution, and data selection criteria. In  
85 addition, we use this dataset to assess the performance of isotope-enable AGCMs as  
86 an example of its potential applications.

## 87 **2 Description of the Antarctic surface snow isotopic dataset**

### 88 **2.1 Data collections and sources**

89 The Antarctic surface snow isotopic data were collected from published papers and  
90 public data portals. When the raw data used in the published studies were not publicly  
91 available, we requested the data from the authors. We received strong support in the  
92 process of data collection. Figure 1a shows the data points in the original MD08  
93 dataset. Figure 1b shows our newly added observation points (794 new data points),  
94 and Figure 1c shows the total sampling points (1867 data locations) of our updated  
95 dataset.

96 Traverse sampling is an important way to obtain spatially distributed data of  
97 isotopic composition. Therefore, the new data mainly came from different route  
98 traverses (Fig. 2). In particular, over the Dronning Maud Land (DML) (from 0 to  
99 60°E), we compiled the water isotope data from the Swedish–Japanese traverse  
100 between Syowa Station and Dome F Station (Touzeau et al., 2016), the Japanese  
101 Antarctic Research traverse (Uemura et al., 2016), the Coldest Firm (CoFi) project  
102 traverse from Kohnen Station to Plateau Station (Weinhart et al., 2021), and the

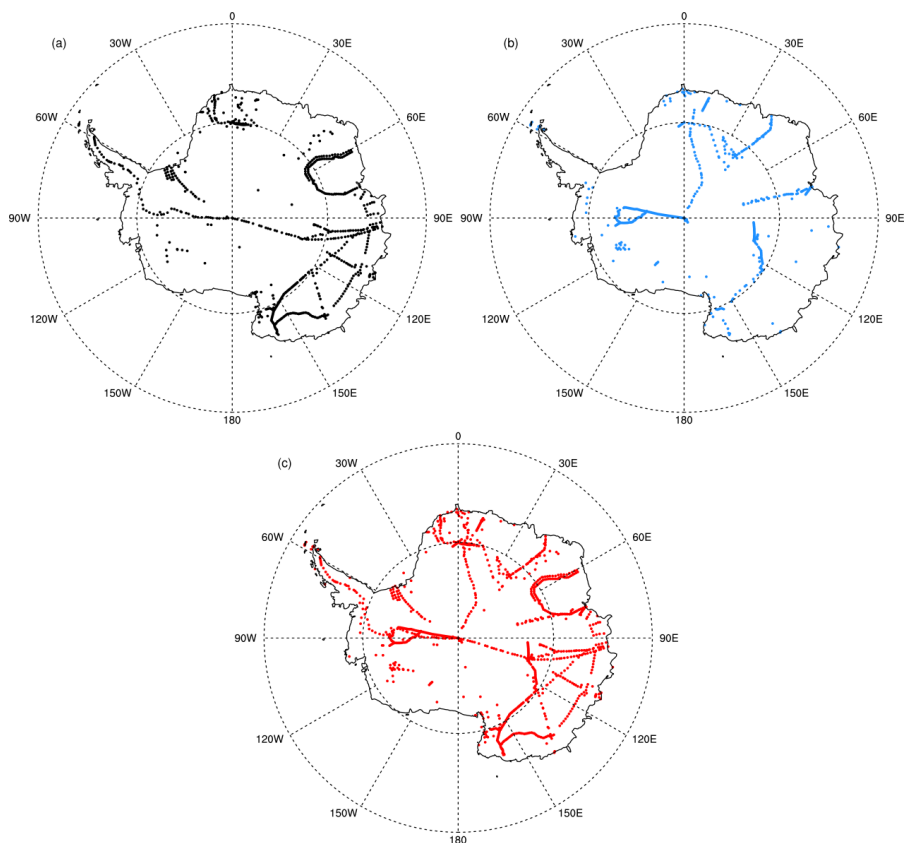


5

103 Spanish expedition from Novolazarevskaja Station to South Pole Station (Landais et al.,  
104 2017). Our dataset also included published records from the Chinese traverse from  
105 Zhongshan Station to Dome A, near the Lambert Glacier (Li et al., 2014, 2021). For  
106 the high inland region of East Antarctica (90 to 120°E), we added two routes of  
107 traverse data (Vostok–Dome B and Vostok–Dome C traverses). Furthermore, in the  
108 area around the Vostok site, we included 89 unreleased public snow pits data, such as  
109 the Vostok flow line data (Ekaykin et al., 2012). Previous data over the West  
110 Antarctica Ice Sheet (WAIS) area mainly came from the International  
111 Trans-Antarctica Scientific Expeditions (Qin et al., 1994; Steig et al., 2005). The  
112 updated dataset includes more recent traverses of the WAIS by Brazilian and Chilean  
113 researchers from the Möller Ice Stream (MIS) basin to the Pine Island Glacier (PIG)  
114 basin (Marcher et al., 2022), and from Patriot Hills to South Pole (Marquette et al.,  
115 2015). It also includes the Satellite Era Accumulation Traverse (SEAT) firn core data  
116 collected during the 2010–2012 field season on the WAIS ice divide (Burgener et al.,  
117 2013; Williams, 2013).



6



118

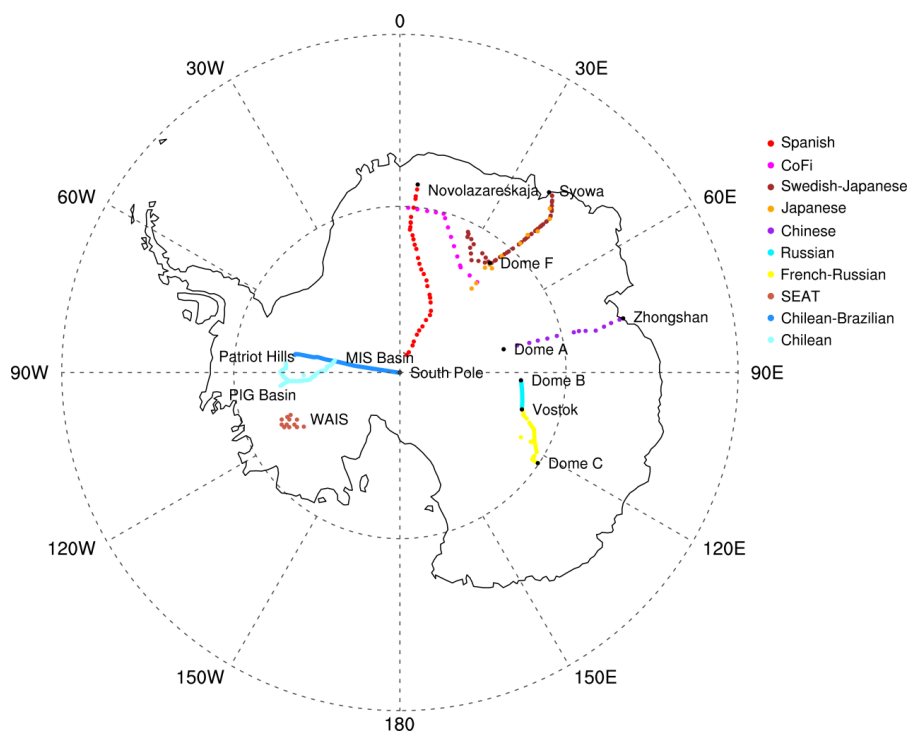
119 Figure 1. The comprehensive dataset of Antarctic surface snow isotopic observations.

120 The black points indicate the original dataset of MD08 (a), and the blue points

121 represent our newly added points (b), and the red points indicate all data locations (c).



7



122

123 Figure 2. Major new sampling traverses of isotopic observations in Antarctica.

124

125 **2.2 Selection criteria and types of data collected in the Antarctic surface snow**  
126 **isotopic dataset**

127 We applied strict data selection criteria to ensure consistent quality over the entire  
128 dataset. As we aimed for a reliable isotopic dataset of multi-year averages, we  
129 excluded isotopic data with apparent seasonal bias and those modified by  
130 post-depositional processes. For example, previous studies reported a high number of  
131 surface snow samples with negative d-excess values in the Dry Valleys (Gooseff et al.,  
132 2006; MD08; Hu et al., 2022). They likely came from fresh surface snow or surface  
133 glacial ice, which could not represent the multi-year average isotope values. Therefore,  
134 we excluded these surface samples from the Dry Valleys (Gooseff et al., 2006;  
135 MD08), and only retained data from snow pits. For snow pits and shallow firn ice



8

136 cores, data should contain at least one-year's record. For longer ice cores, only data of  
137 the last few decades were included. For precipitation, data should cover at least one  
138 year. For the surface snow, samples should have a thickness adequate to cover a full  
139 year's accumulation. For example, surface snow samples from East Antarctic coastal  
140 sites should have a depth of at least 30 cm, while those from central West Antarctic  
141 Ice Sheet should have a depth of at least 15–20 cm. Data were averaged at each site to  
142 get the multi-year mean.

### 143 **2.3 Metadata**

144 Table 1 provides a detailed description of metadata fields used in our Antarctic  
145 surface snow isotopic observation dataset. Key information included the site latitude  
146 and longitude, geographic factors (elevation and distance to the nearest coast), climate  
147 conditions (temperature and net snow accumulation rate), and isotopic values.  
148 Latitude and longitude data were provided in the literature or by contributing  
149 researchers. Elevations were extracted from the Global Earth Relief Grids data  
150 (<https://lpdaac.usgs.gov/products/srtmg13v003/>) at a spatial resolution of 0.09 km. We  
151 applied the built-in functions in the Generic Mapping Tools (GMT) software (Wessel  
152 et al., 2019) to calculate distance from the nearest coast. Firn temperature or surface  
153 air temperature data were obtained either from the literature or provided by the  
154 contributing researchers. The net snow accumulation rate, when available, was  
155 expressed in cm w.e. yr<sup>-1</sup>. The dataset contains 1867 data points in total, including  
156 1604 locations for  $\delta^{18}\text{O}$  and 1278 locations for  $\delta^2\text{H}$ , and 1204 positions for both,  
157 where the d-excess (defined as  $\text{d-excess} = \delta^2\text{H} - 8 \times \delta^{18}\text{O}$ ) could be calculated.

158

159 Table 1. Descriptions of metadata fields in the Antarctic surface snow isotopic  
160 observation dataset





9

Field number	Information
1	Sample ID number
2	latitude (decimal degrees)
3	longitude (decimal degrees)
4	site name
5	elevation (m)
6	sampling date
7	sample type
8	reference or source
9	published distance from the nearest coast (km)
10	calculated distance from the nearest coast (km)
11	firn temperature or surface air temperature (°C)
12	accumulation of snow/ice per year (cm w.e./yr)
13	averaging length (years or depth)
14	Number of averaged values
15	mean $\delta^2\text{H}$ (traditionally referred to as $\delta\text{D}$ , ‰)
16	min $\delta^2\text{H}$ (‰)
17	max $\delta^2\text{H}$ (‰)
18	$\delta^2\text{H}$ standard deviation (‰)
19	mean $\delta^{18}\text{O}$ (‰)
20	min $\delta^{18}\text{O}$ (‰)
21	max $\delta^{18}\text{O}$ (‰)
22	$\delta^{18}\text{O}$ standard deviation (‰)
23	mean d-excess (‰)



1

24	max d-excess (‰)
25	min d-excess (‰)
26	d-excess standard deviation (‰)
27	calculated elevation (m)
28	place of measurements (country)
29	original quality control:  (1) analytical uncertainty of 0.1‰ or better for $\delta^{18}\text{O}$ measurements,  (2) analytical uncertainty of 1.0‰ or better for $\delta^2\text{H}$ measurements,  (3) sufficient number of measurements (10 or more),  (4) age control on the sampling period or a core depth),  (5) seasonal resolution of the measurements

161 Note: The original quality control index ranging from 0 (minimum quality control) to  
162 5 (maximum quality control).

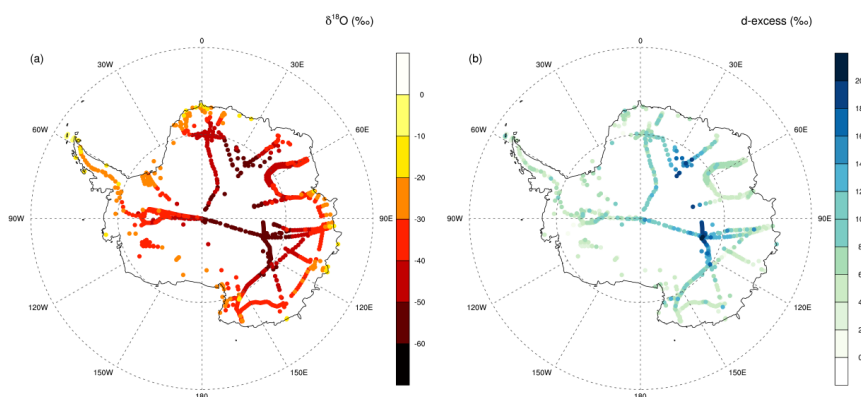
163 **3 Annual mean spatial distribution of Antarctic  $\delta^{18}\text{O}$  and d-excess**  
164 **and evaluation of isotope-incorporated AGCMs**

165 The measured  $\delta^{18}\text{O}$  values range from  $-59.95$  to  $-7.80\text{‰}$ , with the maximum and  
166 minimum values at the Antarctic Peninsula and near Vostok Station respectively (Fig.  
167 3a). The d-excess values range from  $-5.8$  to  $21.8\text{‰}$ , with the minimum and maximum  
168 values in the Dry Valleys and near Vostok Station respectively (Fig. 3b). The spatial  
169 pattern clearly shows the continental effect with the  $\delta^{18}\text{O}$  values decreasing from the



1

170 coast to the interior regions due to the temperature-dependent isotopic distillation (Fig.  
171 4a, 4c, and 4e), and d-excess increasing from the coast to the interior (Fig. 4b, 4d, and  
172 4f) because of the equilibrium and kinetic fractionation effects occurring during the  
173 formation of ice crystals at very low temperatures (Jouzel and Merlivat, 1984). It  
174 should be noted that we do not quantitatively calculate the quantitative relationship  
175 between isotope ratios and geographical and climatic factors here, which is beyond  
176 the scope of this paper.

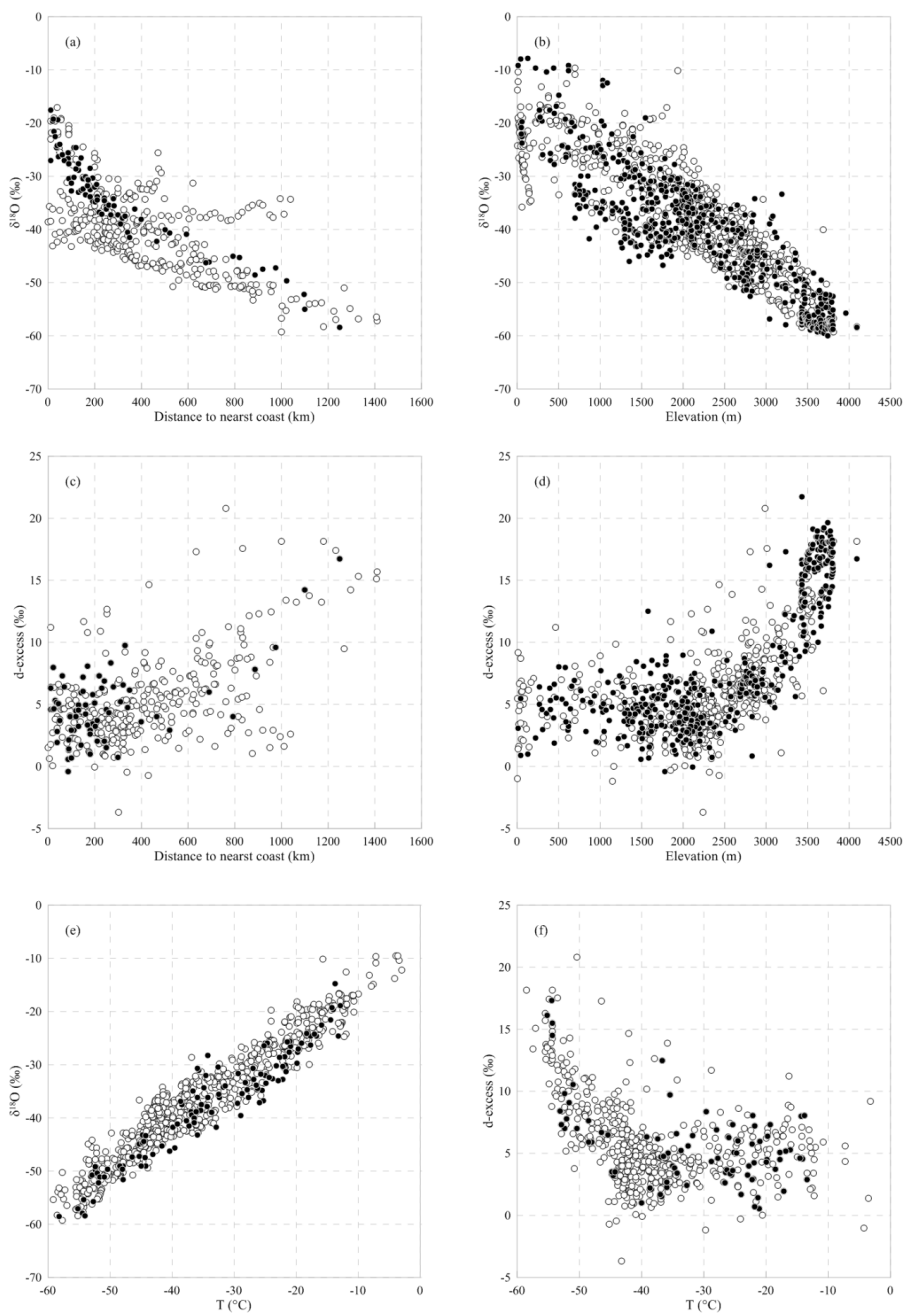


177

178 Figure 3. Spatial distribution of (a)  $\delta^{18}\text{O}$  and (b) d-excess in Antarctic surface snow.



1



179

180 Figure 4. Scatter plots for (a)  $\delta^{18}\text{O}$  vs. distance to the nearest coast and (b)  $\delta^{18}\text{O}$  vs.  
181 elevation. (c) and (d), same as (a) and (b), but for d-excess. (e) Scatter plot for  $\delta^{18}\text{O}$  vs.



1

182 temperature. (f), same as (e), but for d-excess. The open circles indicate the original  
183 data set of MD08, and the filled points represent our newly added points.

184

185 In order to compare our isotopic dataset with the simulations from  
186 isotope-incorporated AGCMs, we used the published results of two recent versions of  
187 isotope-enabled AGCMs: the European Centre for Medium-Range Weather  
188 Forecasting-Hamburg Atmosphere Model equipped with water isotopes, version 6  
189 (ECHAM6-wiso) and the isotope-enabled Community Atmosphere Model, version 6  
190 (iCAM6). The ECHAM6-wiso model was driven by the ERA5 reanalysis dataset  
191 (Hersbach et al., 2020) with a horizontal resolution of  $0.9^\circ \times 0.9^\circ$  for the period 1979  
192 to 2018 (Cauquoin and Werner, 2021). The iCAM6 model was also driven by the  
193 ERA5 and the simulation time spans from 1980 to 2004 with a horizontal resolution  
194 of  $0.9^\circ \times 1.25^\circ$  (Fiorella et al., 2021). These two recent versions of isotope-enabled  
195 AGCMs could well reproduce the spatial distribution characteristics of Antarctic  
196 precipitation  $\delta^{18}\text{O}$  and d-excess (Fig. 5). The correlation coefficient between  
197 measured and observed  $\delta^{18}\text{O}$  is slightly higher for ECHAM6-wiso ( $r = 0.97$ ,  
198 model-data slope = 0.78,  $p < 0.01$ ) than iCAM6 ( $r = 0.96$ , model-data slope = 0.84,  $p$   
199  $< 0.01$ ) (Figs. 5a and 5b, Figs. 5e and 5f). The performance of ECHAM6-wiso in  
200 simulating d-excess ( $r = 0.77$ , model-data slope = 0.22,  $p < 0.01$ ) is significantly  
201 inferior to iCAM6 ( $r = 0.89$ , model-data slope = 1.01,  $p < 0.01$ ) (Figs. 5c and 5d, Figs.  
202 5g and 5h). The iCAM6 was improved over its predecessor iCAM5 in several  
203 significant ways, particularly in its cloud parameterizations (e.g., Bogenschütz et al.,  
204 2018). These changes included a revision to the contact angle distributions (Wang et  
205 al., 2014), how pre-existing ice crystals influence ice nucleation rates (Shi et al.,  
206 2015), and a new prognostic microphysics scheme (Gettelman et al., 2015). Together,

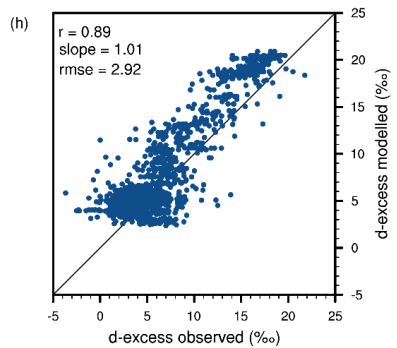
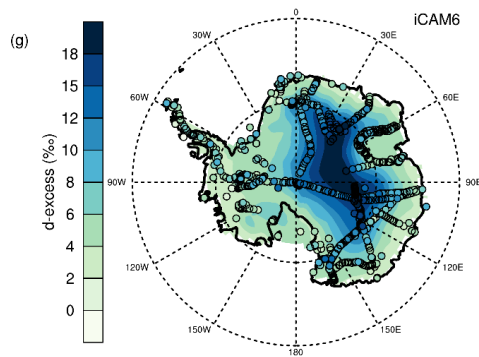
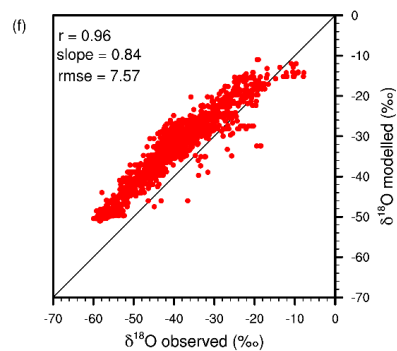
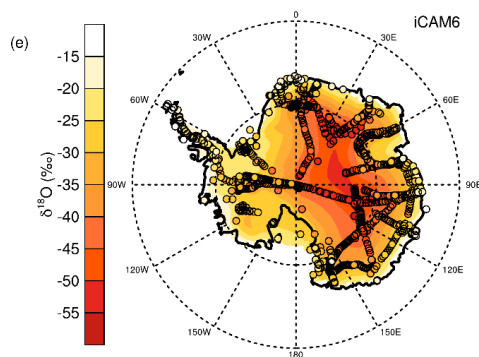
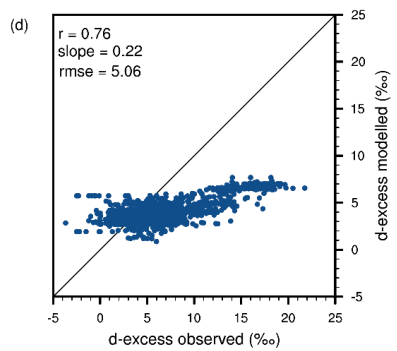
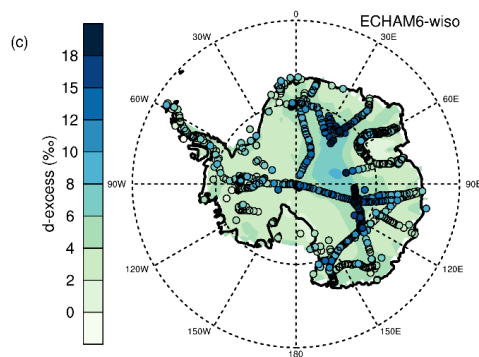
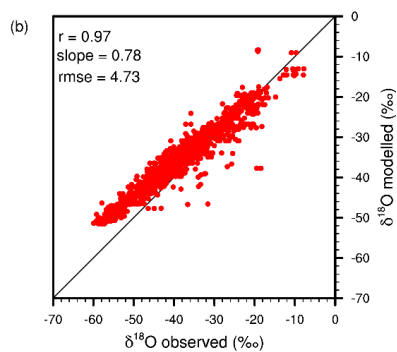
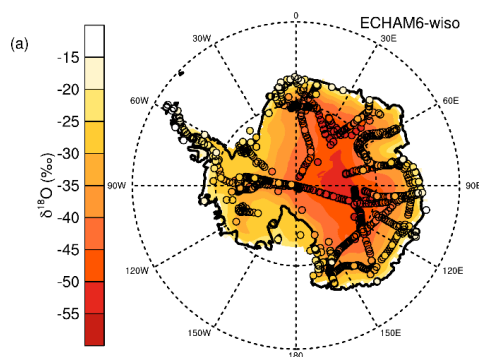


1

207 these changes allowed for lower supersaturation, which led to an increase of the  
208 modeled d-excess in Antarctica by 5–10‰ (see Figure 4 of Fiorella et al. (2021)).  
209 This could explain the iCAM6's better ability to model d-excess of snow and  
210 precipitation in Antarctica in comparison to ECHAM6-wiso. ECHAM6-wiso, when  
211 nudged to the ERA5 reanalyses, significantly underestimated the d-excess in  
212 Antarctic precipitation. This bias was slightly reduced when using the results from a  
213 preindustrial simulation instead (average climatic conditions from 1870 to 1899) ( $r =$   
214  $0.84$ , model-data slope =  $0.31$ ,  $p < 0.01$ , see Supplement Fig. S1). This simulation was  
215 used by Cauquoin and Werner (2021) to re-tune the supersaturation equation used in  
216 ECHAM6-wiso, based on the reproduction of the observed d-excess/ $\delta^2\text{H}$  relationship  
217 from the Antarctic surface snow isotopic dataset of MD08. In conclusion, two recent  
218 versions of isotope-enabled AGCMs were able to reproduce the isotopic composition  
219 of precipitation and snow in Antarctica. This information could give us more  
220 confidence in using these water isotope simulations in polar regions for paleoclimate  
221 reconstruction.



1





1

223 Figure 5. Comparisons of observational water isotopes data with the ECHAM6-wiso  
224 and iCAM6 simulations. (a) The observational  $\delta^{18}\text{O}$  (filled circles) and the simulated  
225  $\delta^{18}\text{O}$  (background color ramp) by ECHAM6-wiso model. (b) Scatter plot of the  
226 simulated  $\delta^{18}\text{O}$  (y-axis) vs. observational  $\delta^{18}\text{O}$  (x-axis). (c) and (d), same as (a) and  
227 (b), but for d-excess. (e) and (f), same as (a) and (b), but for iCAM6. (g) and (h), same  
228 as (e) and (f), but for d-excess. Letter r represents the correlation coefficient, slope  
229 represents the slope of linear regression, and rmse represents the root mean square  
230 error.

#### 231 **4 Data availability**

232 The updated Antarctic surface snow isotopic dataset used in this article is available  
233 at <https://doi.org/10.5281/zenodo.7294183> (Wang et al., 2022).

#### 234 **5 Conclusions and outlook**

235 We compiled a multi-year-averaged Antarctic surface snow isotopic dataset by  
236 integrating a previous database with more recent observations. This dataset greatly  
237 improved the spatial coverage of isotopic observations in Antarctica. As an example  
238 of its potential applications, we made a comparison between the isotopic observation  
239 data and the simulation results from the two most recent isotope-enabled AGCMs.  
240 The results show that the ECHAM6-wiso and iCAM6 in general captured the spatial  
241 variation and characteristics of Antarctic precipitation isotopes. The updated dataset  
242 has many important potential applications in investigating spatial variability and the  
243 climatology of water isotopes in the region, evaluating models, and interpreting  
244 Antarctic ice core records for past climate variations.





1

245 For better data integration and update, we make the following recommendations for  
246 future studies: (1) more data are needed at high elevations in interior Antarctica; (2)  
247 data collection techniques such as dual-tube sampling are needed to ensure annual  
248 data coverage and reduce seasonal biases; (3) all isotopic observation data should be  
249 made publicly available. Finally, we look forward to collaborating with a wide range  
250 of researchers to update and refine this dataset on regular basis.

251

252 **Supplement.** GMT programs include DEM data that calculate the distance to the  
253 nearest coast and extracts the site's elevation.

254 **Author contributions.** HP and SH initiated the project leading to the collection  
255 of the Antarctic surface snow isotopic dataset. JW was responsible for collecting and  
256 collating all the data, as well as completing the first draft of the article. The original  
257 draft was improved by SW, SWS, RU, AE, MW, AC, SGO, and SR. HP and SH  
258 supervised this work. All authors contributed to the final form of the manuscript.

259 **Competing interests.** The authors declare that they have no conflict of interest.

260 **Acknowledgements.**

261 This work was jointly supported by the National Natural Science Foundation of China  
262 (41622605, 41830644, and 91837102), the Priority Academic Program Development  
263 of Jiangsu Higher Education Institutions (PAPD), the Collaborative Innovation Center  
264 of Climate Change of Jiangsu Province of China, the Fundamental Research Funds  
265 for the Central Universities (020914380190), and the ERC Starting Grant  
266 COMBINISO (306045). We thank Jean-Louis Tison for his support and Jesse  
267 Nusbaumer for the interpretation of the iCAM6 results. We are grateful for the help of



1

268 Jean Jouzel and Jiandong Xu. Finally, we thank the scientists who have provided help  
269 and support in data collection.

270

## 271 **References:**

272 Bogenschutz, P. A., Gettelman, A., Hannay, C., Larson, V. E., Neale, R. B., Craig, C.,  
273 and Chen, C.-C.: The path to CAM6: coupled simulations with CAM5.4 and  
274 CAM5.5, *Geosci. Model Dev.*, 11, 235–255,  
275 <https://doi.org/10.5194/gmd-11-235-2018>, 2018.

276 Brook, E. J. and Buizert, C.: Antarctic and global climate history viewed from ice  
277 cores, *Nature*, 558, 200–208, <https://doi.org/10.1038/s41586-018-0172-5>, 2018.

278 Buizert, C., Fudge, T. J., Roberts, W. H. G., Steig, E. J., Sherriff-Tadano, S., Ritz, C.,  
279 Lefebvre, E., Edwards, J., Kawamura, K., Oyabu, I., Motoyama, H., Kahle, E. C.,  
280 Jones, T. R., Abe-Ouchi, A., Obase, T., Martin, C., Corr, H., Severinghaus, J. P.,  
281 Beaudette, R., Epifanio, J. A., Brook, E. J., Martin, K., Chappellaz, J., Aoki, S.,  
282 Nakazawa, T., Sowers, T. A., Alley, R. B., Ahn, J., Sigl, M., Severi, M., Dunbar, N.  
283 W., Svensson, A., Fegyveresi, J. M., He, C., Liu, Z., Zhu, J., Otto-Bliesner, B. L.,  
284 Lipenkov, V. Y., Kageyama, M., and Schwander, J.: Antarctic surface temperature  
285 and elevation during the Last Glacial Maximum, *Science*, 372, 1097–1101,  
286 <https://doi.org/10.1126/science.abd2897>, 2021.

287 Cauquoin, A. and Werner, M.: High-Resolution Nudged Isotope Modeling With  
288 ECHAM6-Wiso: Impacts of Updated Model Physics and ERA5 Reanalysis Data, *J*  
289 *Adv Model Earth Syst*, 13, <https://doi.org/10.1029/2021MS002532>, 2021.

290 Dütch, M., Blossey, P. N., Steig, E. J., and Nusbaumer, J. M.: Nonequilibrium  
291 Fractionation During Ice Cloud Formation in iCAM5: Evaluating the Common  
292 Parameterization of Supersaturation as a Linear Function of Temperature, *J Adv*  
293 *Model Earth Syst*, 11, 3777–3793, <https://doi.org/10.1029/2019MS001764>, 2019.

294 Ekaykin, A. A., Bolshunov, A. V., Lipenkov, V. Ya., Scheinert, M., Eberlein, L.,  
295 Brovko, E., Popov, S. V., and Turkeev, A. V.: First glaciological investigations at



1

- 296 Ridge B, central East Antarctica, *Antarctic Science*, 33, 418–427,  
297 <https://doi.org/10.1017/S0954102021000171>, 2021.
- 298 Ekaykin, A. A., Lipenkov, V. Ya., and Shibaev, Yu. A.: Spatial distribution of the  
299 snow accumulation rate along the ice flow lines between Ridge B and Lake Vostok,  
300 *Journal of Ice and Snow*, 52, 122,  
301 <https://doi.org/10.15356/2076-6734-2012-4-122-128>, 2012.
- 302 Fiorella, R. P., Siler, N., Nusbaumer, J., and Noone, D. C.: Enhancing Understanding  
303 of the Hydrological Cycle via Pairing of Process-Oriented and Isotope Ratio  
304 Tracers, *J Adv Model Earth Syst*, 13, <https://doi.org/10.1029/2021MS002648>,  
305 2021.
- 306 Gettelman, A. and Morrison, H.: Advanced Two-Moment Bulk Microphysics for  
307 Global Models. Part I: Off-Line Tests and Comparison with Other Schemes,  
308 *Journal of Climate*, 28, 1268–1287, <https://doi.org/10.1175/JCLI-D-14-00102.1>,  
309 2015.
- 310 Hatvani, I. G., Leuenberger, M., Kohón, B., and Kern, Z.: Geostatistical analysis and  
311 isoscape of ice core derived water stable isotope records in an Antarctic macro  
312 region, *Polar Science*, 13, 23–32, <https://doi.org/10.1016/j.polar.2017.04.001>, 2017.
- 313 Hersbach, H., Bell, B., Berrisford, P., Hirahara, S., Horányi, A., Muñoz-Sabater, J.,  
314 Nicolas, J., Peubey, C., Radu, R., Schepers, D., Simmons, A., Soci, C., Abdalla, S.,  
315 Abellan, X., Balsamo, G., Bechtold, P., Biavati, G., Bidlot, J., Bonavita, M., De  
316 Chiara, G., Dahlgren, P., Dee, D., Diamantakis, M., Dragani, R., Flemming, J.,  
317 Forbes, R., Fuentes, M., Geer, A., Haimberger, L., Healy, S., Hogan, R. J., Hólm,  
318 E., Janisková, M., Keeley, S., Laloyaux, P., Lopez, P., Lupu, C., Radnoti, G., De  
319 Rosnay, P., Rozum, I., Vamborg, F., Villaume, S., and Thépaut, J.-N.: The ERA5  
320 global reanalysis, *Q. J. Roy. Meteor. Soc.*, 146, 1999–2049,  
321 <https://doi.org/10.1002/qj.3803>, 2020.
- 322 Hu, J., Yan, Y., Yeung, L. Y., and Dee, S. G.: Sublimation Origin of Negative  
323 Deuterium Excess Observed in Snow and Ice Samples From McMurdo Dry Valleys



2

- 324 and Allan Hills Blue Ice Areas, East Antarctica, *J. Geophys. Res. Atmos.*, 127,  
325 <https://doi.org/10.1029/2021JD035950>, 2022.
- 326 Hurrell, J. W., Hack, J. J., Shea, D., Caron, J. M., and Rosinski, J.: A New Sea  
327 Surface Temperature and Sea Ice Boundary Dataset for the Community  
328 Atmosphere Model, *Journal of Climate*, 21, 5145–5153,  
329 <https://doi.org/10.1175/2008JCLI2292.1>, 2008.
- 330 Jouzel, J. and Merlivat, L.: Deuterium and oxygen 18 in precipitation: Modeling of  
331 the isotopic effects during snow formation, *J. Geophys. Res.*, 89, 11749,  
332 <https://doi.org/10.1029/JD089iD07p11749>, 1984.
- 333 Jouzel, J., Masson-Delmotte, V., Cattani, O., Dreyfus, G., Falourd, S., Hoffmann, G.,  
334 Minster, B., Nouet, J., Barnola, J. M., Chappellaz, J., Fischer, H., Gallet, J. C.,  
335 Johnsen, S., Leuenberger, M., Loulergue, L., Luethi, D., Oerter, H., Parrenin, F.,  
336 Raisbeck, G., Raynaud, D., Schilt, A., Schwander, J., Selmo, E., Souchez, R.,  
337 Spahni, R., Stauffer, B., Steffensen, J. P., Stenni, B., Stocker, T. F., Tison, J. L.,  
338 Werner, M., and Wolff, E. W.: Orbital and Millennial Antarctic Climate Variability  
339 over the Past 800,000 Years, *Science*, 317, 793–796,  
340 <https://doi.org/10.1126/science.1141038>, 2007.
- 341 Landais, A., Casado, M., Prié, F., Magand, O., Arnaud, L., Ekaykin, A., Petit, J.-R.,  
342 Picard, G., Fily, M., Minster, B., Touzeau, A., Goursaud, S., Masson-Delmotte, V.,  
343 Jouzel, J., and Orsi, A.: Surface studies of water isotopes in Antarctica for  
344 quantitative interpretation of deep ice core data, *Comptes Rendus Geoscience*, 349,  
345 139–150, <https://doi.org/10.1016/j.crte.2017.05.003>, 2017.
- 346 Li, C., Kang, S., Shi, G., Huang, J., Ding, M., Zhang, Q., Zhang, L., Guo, J., Xiao, C.,  
347 Hou, S., Sun, B., Qin, D., and Ren, J.: Spatial and temporal variations of total  
348 mercury in Antarctic snow along the transect from Zhongshan Station to Dome A,  
349 *Tellus B: Chemical and Physical Meteorology*, 66, 25152,  
350 <https://doi.org/10.3402/tellusb.v66.25152>, 2014.
- 351 Li, C., Ren, J., Shi, G., Pang, H., Wang, Y., Hou, S., Li, Z., Du, Z., Ding, M., Ma, X.,  
352 Yang, J., Xie, A., Wang, P., Wang, X., Sun, B., and Xiao, C.: Spatial and temporal  
353 variations of fractionation of stable isotopes in East-Antarctic snow, *J. Glaciol.*, 67,  
354 523–532, <https://doi.org/10.1017/jog.2021.5>, 2021.
- 355 Marcher, A., Bernardo, R. T., Simões, J. C., and Auger, J.: Water stable isotopes in  
356 snow along a traverse of the West Antarctic Ice Sheet: insights into moisture



2

- 357 origins, air-masses distillation history, and climatic value, *An. Acad. Bras. Ciênc.*,  
358 94, e20210353, <https://doi.org/10.1590/0001-376520220210353>, 2022.
- 359 Marquette, L., Simões, J. C., Casassa, G., Introne, D. S., and Dos Santos, E. A.:  
360 Variações na composição isotópica de oxigênio na neve superficial ao longo de  
361 uma travessia antártica, *Pesq Geoc*, 42, 227,  
362 <https://doi.org/10.22456/1807-9806.78122>, 2015.
- 363 Masson-Delmotte, V., Hou, S., Ekaykin, A., Jouzel, J., Aristarain, A., Bernardo, R. T.,  
364 Bromwich, D., Cattani, O., Delmotte, M. M., Falourd, S., Frezzotti, M., Gallée, H.,  
365 Genoni, L., Isaksson, E., Landais, A., Helsen, M. M., Hoffmann, G., Lopez, J.,  
366 Morgan, V., Motoyama, H., Noone, D., Oerter, H., Petit, J. R., Royer, A., Uemura,  
367 R., Schmidt, G. A., Schlosser, E., Simões, J. C., Steig, E. J., Stenni, B., Stievenard,  
368 M., Van Den Broeke, M. R., Van De Wal, R. S., Van De Berg, W. J., Vimeux, F.,  
369 and White, J. W.: A review of antarctic surface snow isotopic composition:  
370 Observations, atmospheric circulation, and isotopic modeling, *J. Climate*, 21,  
371 3359–3387, <https://doi.org/10.1175/2007JCLI2139.1>, 2008.
- 372 Medley, B. and Thomas, E. R.: Increased snowfall over the Antarctic Ice Sheet  
373 mitigated 20th century sea-level rise, *Nat. Clim. Change*, 9, 34–39,  
374 <https://doi.org/10.1038/s41558-018-0356-x>, 2019.
- 375 Naughten, K. A., De Rydt, J., Rosier, S. H. R., Jenkins, A., Holland, P. R., and Ridley,  
376 J. K.: Two-timescale response of a large Antarctic ice shelf to climate change, *Nat*  
377 *Commun*, 12, 1991, <https://doi.org/10.1038/s41467-021-22259-0>, 2021.
- 378 Shi, X., Liu, X., and Zhang, K.: Effects of pre-existing ice crystals on cirrus clouds  
379 and comparison between different ice nucleation parameterizations with the  
380 Community Atmosphere Model (CAM5), *Atmos. Chem. Phys.*, 15, 1503–1520,  
381 <https://doi.org/10.5194/acp-15-1503-2015>, 2015.
- 382 Stokes, C. R., Abram, N. J., Bentley, M. J., Edwards, T. L., England, M. H., Foppert,  
383 A., Jamieson, S. S. R., Jones, R. S., King, M. A., Lenaerts, J. T. M., Medley, B.,  
384 Miles, B. W. J., Paxman, G. J. G., Ritz, C., van de Flierdt, T., and Whitehouse, P.



2

- 385 L.: Response of the East Antarctic Ice Sheet to past and future climate change,  
386 Nature, 608, 275–286, <https://doi.org/10.1038/s41586-022-04946-0>, 2022.
- 387 Touzeau, A., Landais, A., Stenni, B., Uemura, R., Fukui, K., Fujita, S., Guilbaud, S.,  
388 Ekaykin, A., Casado, M., Barkan, E., Luz, B., Magand, O., Teste, G., Le Meur, E.,  
389 Baroni, M., Savarino, J., Bourgeois, I., and Risi, C.: Acquisition of isotopic  
390 composition for surface snow in East Antarctica and the links to climatic  
391 parameters, *The Cryosphere*, 10, 837–852, <https://doi.org/10.5194/tc-10-837-2016>,  
392 2016.
- 393 Uemura, R., Masaka, K., Fukui, K., Iizuka, Y., Hirabayashi, M., and Motoyama, H.:  
394 Sulfur isotopic composition of surface snow along a latitudinal transect in East  
395 Antarctica: Isotopic Values of Sulfate in Antarctica, *Geophys. Res. Lett.*, 43, 5878–  
396 5885, <https://doi.org/10.1002/2016GL069482>, 2016.
- 397 Wang, J., Pang, H., and Hou, S.: Antarctic surface snow isotopic dataset (Version 3)  
398 [Data set], Zenodo, <https://doi.org/10.5281/zenodo.7294183>, 2022.
- 399 Wang, Y., Hou, S., Grigholm, B., and Song, L.: An improved method for modeling  
400 spatial distribution of  $\delta D$  in surface snow over Antarctic ice sheet. *Chin. Geogr. Sci.*,  
401 19, 120–125, <https://doi.org/10.1007/s11769-009-0120-2>, 2009b.
- 402 Wang, Y., Hou, S., Masson-Delmotte, V., and Jouzel, J.: A generalized additive  
403 model for the spatial distribution of stable isotopic composition in Antarctic surface  
404 snow. *Chemical Geology*, 271, 133–141,  
405 <https://doi.org/10.1016/j.chemgeo.2010.01.004>, 2010.
- 406 Wang, Y., Hou, S., Masson-Delmotte, V., and Jouzel, J.: A new spatial distribution  
407 map of  $\delta^{18}O$  in Antarctic surface snow. *Geophys. Res. Lett.*, 36,  
408 <https://doi.org/10.1029/2008GL036939>, 2009a.
- 409 Wang, Y., Liu, X., Hoose, C., and Wang, B.: Different contact angle distributions for  
410 heterogeneous ice nucleation in the Community Atmospheric Model version 5,  
411 *Atmos. Chem. Phys.*, 14, 10411–10430, <https://doi.org/10.5194/acp-14-10411-2014>,  
412 2014.
- 413 Weinhart, A. H., Kipfstuhl, S., Hörhold, M., Eisen, O., and Freitag, J.: Spatial  
414 Distribution of Crusts in Antarctic and Greenland Snowpacks and Implications for



2

- 415 Snow and Firn Studies, *Front. Earth Sci.*, 9, 630070,  
416 <https://doi.org/10.3389/feart.2021.630070>, 2021.
- 417 Werner, M., Jouzel, J., Masson-Delmotte, V., and Lohmann, G.: Reconciling glacial  
418 Antarctic water stable isotopes with ice sheet topography and the isotopic  
419 paleothermometer, *Nat Commun*, 9, 3537,  
420 <https://doi.org/10.1038/s41467-018-05430-y>, 2018.
- 421 Wessel, P., Luis, J. F., Uieda, L., Scharroo, R., Wobbe, F., Smith, W. H. F., and Tian,  
422 D.: The Generic Mapping Tools Version 6, *Geochem. Geophys. Geosyst.*, 20,  
423 5556–5564, <https://doi.org/10.1029/2019GC008515>, 2019.
- 424 Williams, J.: Toward a Better Understanding of Recent Warming of the Central West  
425 Antarctic Ice Sheet from Shallow Firn Cores, 2013.
- 426
- 427
- 428